The Astrophysical Journal Letters, 823:L37 (4pp), 2016 June 1 doi:10.3847/2041-8205/823/2/L37

EXPLORATORY *CHANDRA* OBSERVATION OF THE ULTRALUMINOUS QUASAR SDSS J010013.02+280225.8 AT REDSHIFT 6.30

Yanli Ai[1], Liming Dou[2], Xiaohui Fan[3,4], Feige Wang[5], Xue-Bing Wu[4,5], and Fuyan Bian[6,7]
[1] School of Physics and Astronomy, Sun Yat-Sen University, Guangzhou 510275, China; aiyanli@mail.sysu.edu.cn
[2] Key Laboratory for Research in Galaxies and Cosmology, Astronomy Department, The University of Sciences and Technology of China, Hefei, Anhui 230026, China
[3] Steward Observatory, University of Arizona, 933 North Cherry Avenue, Tucson, AZ 85721, USA
[4] Kavli Institute for Astronomy and Astrophysics, Peking University, Beijing 100871, China
[5] Department of Astronomy, School of Physics, Peking University, Beijing 100871, China
[6] Research School of Astronomy and Astrophysics, Australian National University, Weston Creek, ACT 2611, Australia
Received 2016 April 13; revised 2016 May 10; accepted 2016 May 16; published 2016 June 1

ABSTRACT

We report exploratory *Chandra* observations of the ultraluminous quasar SDSS J010013.02+280225.8 at redshift 6.30. The quasar is clearly detected by *Chandra* with a possible component of extended emission. The rest-frame 2–10 keV luminosity is $9.0^{+9.1}_{-4.5} \times 10^{45}$ erg s^{-1} with an inferred photon index of $\Gamma = 3.03^{+0.78}_{-0.70}$. This quasar is X-ray bright, with an inferred X-ray-to-optical flux ratio $\alpha_{ox} = -1.22^{+0.07}_{-0.05}$, higher than the values found in other quasars of comparable ultraviolet luminosity. The properties inferred from this exploratory observation indicate that this ultraluminous quasar might be growing with super-Eddington accretion and probably viewed with a small inclination angle. Deep X-ray observations will help to probe the plausible extended emission and better constrain the spectral features for this ultraluminous quasar.

Key words: quasars: individual (SDSS J010013.02+280225.8)

1. INTRODUCTION

A large number of quasars at redshifts of $z \gtrsim 6$ have been discovered, selected with a combination of optical and near-infrared colors (Mortlock et al. 2011; Venemans et al. 2013; Jiang et al. 2015; Wang et al. 2016). These sources are powerful probes of cosmic reionization (Fan et al. 2006) and offer insights into the process by which massive black holes formed and grew in the early universe. Recently, Wu et al. (2015) reported the discovery of SDSS J010013.02+280225.8 (hereafter J0100+2802), an ultraluminous quasar with an estimated black hole mass of 12 billion solar masses. With the highest black hole mass and the highest luminosity among all quasars discovered at $z \gtrsim 5$, it sets the tightest constraints on models for massive black hole growth and evolution at early epochs (e.g., Shankar et al. 2009; Volonteri 2010).

X-ray emissions from quasars reveal the conditions in the innermost regions of their accretion-disk corona, and provide information about how the black hole is fed. There are tentative evidences that high-redshift quasars have relatively soft X-ray spectra, indicating that the black holes are accreting near or above the Eddington rate (Grupe et al. 2006; Page et al. 2014), although debates exist (e.g., Just et al. 2007; Moretti et al. 2014). Mildly super-Eddington intermittent accretion may significantly ease the problem of assembling the massive black holes when the universe was young (Madau et al. 2014). Furthermore, high-redshift quasars, such as the known blazars at $z > 5$ (Romani et al. 2004; Frey et al. 2010; Sbarrato et al. 2013; Ghisellini et al. 2015), may have powerful jets that provide a means by which the black hole accretes at a rate that breaks the Eddington limit (Ghisellini et al. 2013). The extended lobes produced by jets may be strong in X-ray, rather than in radio, as the dramatic $(1 + z)^4$ boosts in the energy density of the cosmic microwave background (CMB) cause inverse Compton scattering to dominate energy loss of relativistic electrons (Fabian et al. 2014).

X-ray observations of J0100+2802 provide a crucial test for understanding the formation of the most massive black holes in the early universe. In this Letter we report our exploratory *Chandra* observation of this ultraluminous quasar. Throughout this paper, we adopt the ΛCDM cosmology parameters from the Planck Collaboration (2014): $\Omega_M = 0.315$, $\Omega_\Lambda = 0.685$, and $H_0 = 67.3$ km s^{-1}. We define power-law photon index Γ such that $N(E) \propto E^{-\Gamma}$. For the Galactic absorption of SDSS J0100+2802, which is included in the model fitting, we use the value of $N_H = 5.82 \times 10^{20}$ cm^{-2} (Kalberla et al. 2005). All uncertainties are given at 1σ, unless otherwise specified.

2. *CHANDRA* OBSERVATION AND DATA ANALYSIS

We obtained *Chandra* observation of SDSS J0100+2802 on 2015 October 16 using the Advanced CCD Imaging Spectrometer (ACIS, Garmire et al. 2003) instrument. The total integration time is 14.8 ks. The target was positioned on the ACIS-S3 chip, which was operated in time-exposure mode, with faint telemetry format. The data were processed with standard CIAO version 4.7 (Fruscione et al. 2006), and only events with grades of 0, 2, 3, 4, and 6 were considered in the analysis. No background flares are present in the observation. We restrict the data to the derived X-ray counts in the observed frame of 0.5–7 keV, considering the increasingly uncertain quantum efficiency of ACIS at lower energies and the steeply increasing background at higher energies.

We first carried out source detection with CIAO task WAVDETECT using wavelet transforms (with wavelet scale sizes of 1, 2, 4, 8, and 16 pixels) and a false-positive probability threshold of 10^{-6}. The quasar is detected at equatorial coordinates of 01:00:13.038, +28:02:25.75. The X-ray position differs from its optical position by 0.1 arcsec, within the radius (0.6 arcsec) of 90% uncertainty circle of *Chandra* ACIS

[7] Stromlo Fellow.

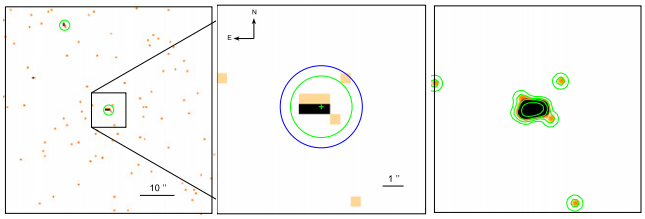

Figure 1. Detection of X-ray emission of J0100+2802. Left: $1' \times 1'$ *Chandra* image centered on J0100+2802 in 0.5–7 keV. The circles show the two sources detected by CIAO task WAVDETECT; Middle: central $10'' \times 10''$ of the image. The plus sign shows the optical position given by SDSS. 14 counts are detected in the 3 pixel radius aperture (green), and one more count in the 4 pixel radius aperture (blue). Right: rebinned image in the middle panel to 0.1 ACIS pixel and smoothed with a $0\farcs492$ Gaussion filter. The size of the ACIS CCD pixel is $\sim 0\farcs492$.

absolute position.[8] At a distance of $28''$ to the northeast of J0100+2802, an X-ray source is detected with 7.9 ± 2.8 net counts (Figure 1). This source is classified as a galaxy in the SDSS DR12 catalog with a photometric redshift of 0.52 ± 0.13 (Alam et al. 2015), therefore it is likely to be a low-luminosity active galactic nucleus in the foreground.

In the image rebinned to 0.1 ACIS pixels and smoothed with a $0\farcs492$ Gaussian filter, the spatial distribution for J0100 +2802 appears somewhat elongated (Figure 1). To measure the extension of this source we use Ciao tool "srcextent." While no conclusive result is returned due to the limited source counts of 14–15. We then manually extracted the photometry of J0100 +2802 and found 14 counts within a 3 pixel ($\sim 1\farcs5$) radius aperture, which corresponds to 94.7% and 89.2% of the encircled energy fraction in 0.5–2 keV and 2–7 keV, respectively.[9] There is one more count detected at an energy of 1.73 keV within the 4 pixel radius aperture (Figure 1). According to the point-spread function at the source position, the expected count in Poisson statistics is 0.16 in the annulus with radii of 3 and 4 pixels, and 0.78 outside of the aperture with radius of 3 pixels. That is, the chance of this photon belonging to the quasar J0100+2802 is 14%–36%. Thus, for J0100+2802 we restrict subsequent analysis to the detected photons within the 3 pixel radius aperture. The average background level, estimated from an annulus in the source position with inner and outer radii of 15 and 20 arcsec, in an aperture of the source size is 0.06 in 0.5–2 keV and 0.05 counts in 2–7 keV.

For J0100+2802, the full-band (0.5–7 keV) X-ray counts are $13.9^{+4.8}_{-3.7}$, with $11.9^{+4.6}_{-3.4}$ in the soft band (0.5–2 keV) and $2.0^{+2.6}_{-1.3}$ in the hard band (2–7 keV). The errors of the X-ray counts were computed according to Gehrels (1986). The hardness ratio, estimated with the Bayesian method[10] (Park et al. 2006), is $-0.78^{+0.07}_{-0.14}$, indicating that the X-ray spectrum of J0100+2802 is soft. The inferred effective photon index from the hardness ratio is indeed large, at $3.2^{+1.0}_{-0.4}$, estimated with Xspec simulation tool "fakeit" and the latest calibration files.

We then perform basic spectral analysis for the quasar. The source spectrum, background spectrum, response matrix files, and auxiliary matrix files are built using the CIAO script SPECEXTRACT. The spectrum is grouped with a minimum of 2 counts per bin. Given that there are only ~14 net counts, we

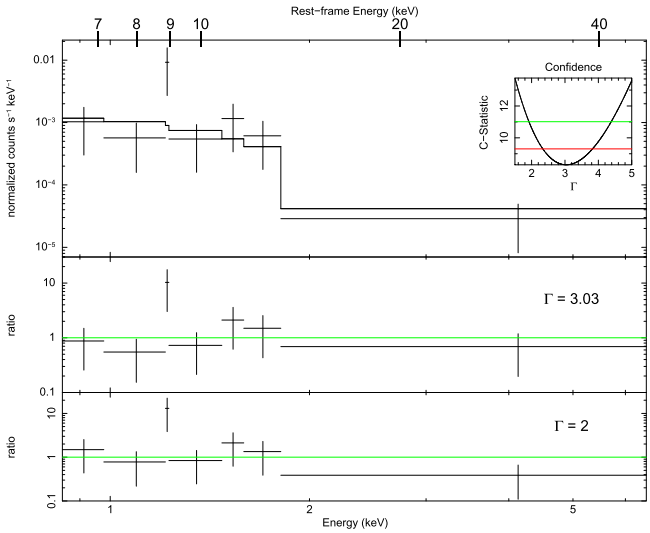

Figure 2. Upper panel: *Chandra* spectrum of J0100+2802 and the best-fit power-law model with $\Gamma = 3.03$ ($N_{\rm H}$ fixed at Galactic $N_{\rm H}^{\rm Gal}$). Inset, confidence curve for the fitted photon index. Middle: data to model ratio of the best-fit model. Significant residual at ~1.2 keV (8.8 keV at rest-frame) is present in the fitting with different photon indices. Lower: data to model ratio, where a power law with fixed $\Gamma = 2.0$ is assumed.

fitted the spectrum using XSPEC (v. 12.9; Arnaud 1996) with a simple power-law model and fixed Galactic absorption. The C-statistic (cstat) was used due to the limited photon counts (Cash 1979). The best-fit photon index is $\Gamma = 3.03^{+0.78}_{-0.70}$, with cstat = 8.31 for 5 degrees of freedom. We also perform simulations taking the exposure time and calibration files, and fit the simulated 1000 spectra. The value of the inferred photon index is consistent with that from the hardness ratio and best fit, with a mean value of 3.13 and a standard deviation of 0.71.

The best-fit results and confidence curve for the photon index are shown in Figure 2. As a comparison, we also show the fitted spectrum with a fixed photon index of 2.0, the typical value found for quasars. From the data to model ratios we can see that the model with a soft spectral index of 3.03 improves the fitting at the most soft and hard energy bands. The rest-frame 2–10 keV luminosity implied by the best fit is $9.0^{+9.1}_{-4.5} \times 10^{45}$ erg s^{-1}. There is a significant residual at ~1.2 keV (8.8 keV at rest-frame). There is no known spectral feature at this energy in quasars, and more counts are needed to investigate the nature of this excess.

We label the detected energy and receiving time of each photon in Figure 3. There are 4 photons detected between 1.207 and 1.228 keV. This unusual feature causes the significant residual at ~1.2 keV in the spectral fitting (Figure 2). Figure 3 also shows the light curve of J0100+2802 with a time bin size of 3 ks. There are 9 photons detected in the first 3 ks bin, while in the middle 6 ks interval no photon is detected, with a 99% confidence upper limit of 4.605 (Gehrels 1986). We first test the variation by analyzing the photon arrival time using the Gregory–Loredo algorithm (Gregory & Loredo 1992) with the CIAO tool GLVARY. The returned variability probability is $P_{\rm GL} = 0.967$, and the variability index is 6 from the test. We then test the chance for a random event of detecting 9 photons in one of the five bins for the total 14 photons with simulation. The chance is 186 in the 10^5 simulated light curves, corresponding to a probability of

[8] http://cxc.cfa.harvard.edu/cal/ASPECT/celmon/
[9] Estimated with the CIAO tool SRC_PSFFRAC.
[10] http://hea-www.harvard.edu/astrostat/behr/

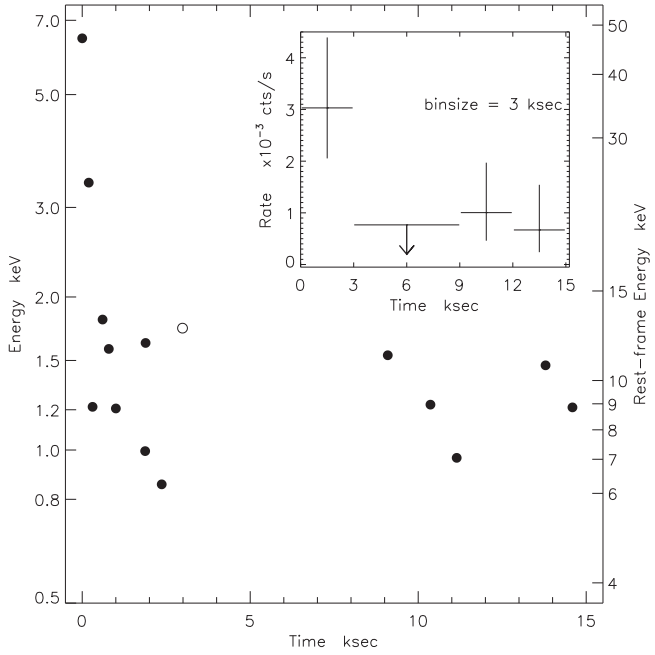

Figure 3. Detected time vs. energy of each photon. The open circle labels the one additional count detected within the 4 pixel radius around the source. Inset, light curve of J0100+2802 in 0.5–7 keV with a time bin size of 3 ks. None of the photons are detected in the middle 6 ks. The 99% confidence upper limit is shown.

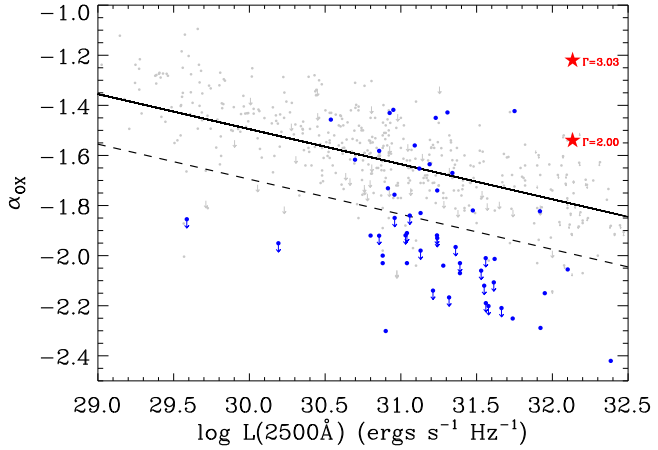

Figure 4. Location of J0100+2802 (red stars) in the X-ray-to-optical power-law slope parameter α_{ox} vs. 2500 Å monochromatic luminosity. The gray dots are the quasars from the samples of Just et al. (2007), Steffen et al. (2006), and Gibson et al. (2008). The blue dots are the weak-line quasars and PHL 1811 analogs from Luo et al. (2015). The solid line represents the Just et al. (2007) α_{ox}–$L_{2500\text{Å}}$ relation, and the dashed line marks the devision between X-ray weak and X-ray normal quasars adopted in Luo et al. (2015). For J0100+2802 the two red stars represent the values of α_{ox} derived with X-ray photon index of 3.03 and 2.0, respectively.

0.019%. Longer exposure observations are needed to investigate this possible variability.

To investigate the broadband properties of J0100+2802 we calculate the X-ray-to-optical spectral energy distribution parameter, α_{ox}, the slope of a nominal power law between 2500 Å and 2 keV in the rest frame ($\alpha_{ox} = 0.384 \times \log(f_{2\,\text{keV}}/f_{2500\,\text{Å}})$, where $f_{2\,\text{keV}}$ is the flux density at 2 keV and $f_{2500\,\text{Å}}$ is the flux density at 2500 Å). For J0100+2802, the rest frame 2500 Å moves to the near-infrared at 18250 Å in the observed frame, falling in the gap between the H and K bands, as shown in Figure 3 in Wu et al. (2015). Using the ultraviolet-optical continuum slope measured in Wu et al. (2015), we estimate the flux density at 2500 Å to be $3.04 \pm 0.45 \times 10^{-16}$ erg s^{-1} cm^{-2} Å^{-1}. An energy of 2 keV in the rest frame of J0100+2802 corresponds to 0.273 keV in the observed frame. This energy is poorly sampled by ACIS. We compute the 0.273 keV flux and the uncertainty from the best-fit power-law model in XSPEC spectral fitting. This yields a value for α_{ox} of $-1.22^{+0.07}_{-0.05}$, with errors dominated by the uncertainty of the rest-frame 2 keV flux.

3. DISCUSSION

The ultraluminous quasar J0100+2802 is strongly detected in our exploratory *Chandra* observation with ∼14 counts. We find the X-ray properties of this quasar to be unusual in several aspects.

First, there is a hint of extended emission, and this feature comes from photons in relatively soft energy bands. As first proposed in Fabian et al. (2014), relativistic electrons in powerful jetted objects with a Lorentz factor of $\Gamma \sim 10^3$ can upscatter CMB photons into the soft X-ray band. Deeper *XMM-Newton* observations, which have a much higher soft X-ray sensitivity compared to *Chandra*, would be ideal to investigate the possibility of this extended emission.

Second, the X-ray spectrum of J0100+2802 is very soft, with an inferred photon index of $3.03^{+0.78}_{-0.70}$, where the mean value of the X-ray photon index found in samples of low- and high-redshift quasars is $1.89 < \langle\Gamma\rangle < 2.19$ (i.e., Wang et al. 2004; Piconcelli et al. 2005; Just et al. 2007; Young et al. 2009). Although there are still debates about whether the X-ray spectrum of high-redshift quasars significantly differs from that of quasars at lower redshifts (Grupe et al. 2006; Just et al. 2007), we note that the highest redshift quasar ULAS J1120+0641 may also exhibit a soft X-ray spectrum with a photon index of $2.6^{+0.4}_{-0.3}$(Page et al. 2014 see Moretti et al. 2014 for a different value of inferred Γ). It has been suggested that the soft X-ray spectrum is an indication that central massive black holes at early epochs are growing at a high accretion rate (Pounds et al. 1995; Leighly 1999).

The inferred Γ can be used as an estimator of L/L_{Edd} by using the linear correlation between Γ and $\log(L/L_{\text{Edd}})$, where L is the bolometric luminosity and L_{Edd} is the Eddington luminosity (Shemmer et al. 2008; Risaliti et al. 2009; Jin et al. 2012; Brightman et al. 2013; Yang et al. 2015). Using different relations presented in the literature, we find that the corresponding L/L_{Edd} for J0100+2802 has a minimum value of 6 (Risaliti et al. 2009), and can be significantly higher (i.e., Shemmer et al. 2008). If those relations did apply to J0100+2802, it could be accreting at significantly above the Eddington rate. Mildly super-Eddington accretion corresponds to a shorter e-folding timescale for black hole mass growth, which can ease the problem of assembling massive black holes out of stellar-mass seeds at early times, even in the case of intermittent accretion (Madau et al. 2014).

Third, J0100+2802 has a relatively high X-ray-to-optical flux ratio compared to those found in other quasars of comparable ultraviolet luminosities (Figure 4). It is well established that the X-ray-to-optical power-law slope parameter α_{ox} of quasars significantly correlate with the ultraviolet 2500 Å monochromatic luminosity ($L_{2500\,\text{Å}}$, Steffen et al. 2006;

Just et al. 2007). According to the α_{ox}–$L_{2500\,Å}$ relation given by Just et al. (2007), a value of $\alpha_{ox} = -1.79 \pm 0.14$ is expected for J0100+2802, compared to be the value of $\alpha_{ox} = -1.22^{+0.07}_{-0.05}$ obtained from the *Chandra* observation. The observed large α_{ox} could be due to the inferred steep X-ray photon index, which is still not well constrained based on the current signal-to-noise ratio of the data. Even if we adopt a flat X-ray spectral shape with an X-ray photon index of a nominal 2.0 to infer the rest-frame 2 keV flux for J0100+2802, the derived α_{ox} is $-1.54^{+0.07}_{-0.05}$, still larger than the average, and is at the upper envelope of the observed α_{ox} values at comparable ultraviolet luminosities (Figure 4). However, the value of α_{ox} for J0100 +2802 is still in the range of the ones found in quasars at low to median redshift, supporting that there is no evolution of α_{ox} with redshift (Brandt et al. 2002; Just et al. 2007; Risaliti & Lusso 2015).

J0100+2802 is a weak-line quasar (WLQ) with a rest-frame equivalent width of Lyα + Nv $\sim$ 10 Å (Wu et al. 2015). WLQs are a subclass of radio-quiet quasars that have extremely weak or almost undetectable emission lines (e.g., Fan et al. 1999; Meusinger & Balafkan 2014 and references therein). The nature of WLQs is still under investigation, although a number of hypotheses have been proposed, such as abnormal broad emission line regions with a significant deficit of line-emitting gas (e.g., Shemmer et al. 2010) or in an early evolutionary stage of formation (e.g., Hryniewicz et al. 2010), a soft ionizing spectral energy distribution due to intrinsic X-ray weakness (e.g., Leighly et al. 2007) or due to small-scale absorption (e.g., Wu et al. 2012; Luo et al. 2015). Significant fractions (~50%) of the WLQs are distinctly X-ray weak compared to typical quasars (Shemmer et al. 2009; Wu et al. 2012; Luo et al. 2015). Our results demonstrate that J0100+2802 is definitely not an X-ray weak WLQ, as shown in Figure 4. If we interpret J0100+2802 in the scenario proposed by Wu et al. (2012) and Luo et al. (2015), in which they unified X-ray weak and X-ray normal WLQs by orientation effects with proposed "shielding-gas," this quasar should be viewed at a small inclination angle.

Finally, we detect a hint of X-ray variability for J0100+2802 within our exposure. For a high-redshift quasar at this luminosity, its X-ray flux is not expected to vary at the timescale of ~10 ks unless beaming is involved. Given that the light crossing time of even the Schwarzschild radius for a 12 billion $M_\odot$ black hole is much longer than 10 ks, the X-ray flux of J0100+2802 is not expected to vary in our observations unless strong beaming is involved. Deeper *XMM-Newton* observations will help to better constrain the spectral features, probe the extended emission, and investigate the variability on both short (~1 hr) and longer (months to year) timescales for this ultraluminous quasar.

Y.-L.A. thanks the support from NSFC grant Nos. 11273060, 11333008, and State Key Development Program for Basic Research of China (Nos. 2013CB834900 and 2015CB857000). F.W. and X.-B.W. thank the support from the NSFC grants No.11373008 and 11533001, the Strategic Priority Research Program "The Emergence of Cosmological Structures" of the Chinese Academy of Sciences, grant No. XDB09000000, and the National Key Basic Research Program of China 2014CB845700. We thank Tinggui Wang, Andy Fabian, Rongfeng Shen, and Yirong Yang and for helpful discussions, and B. Luo for providing the data of Figure 4. This work is based observations made by the *Chandra X-Ray Observatory* and has made use of software provided by the *Chandra* X-Ray Center in the application package CIAO. Support for this work was provided by the National Aeronautics and Space Administration through *Chandra* Award Number GO5-16116B issued by the *Chandra X-ray Observatory* Center, which is operated by the Smithsonian Astrophysical Observatory for and on behalf of the National Aeronautics Space Administration under contract NAS8-03060.

REFERENCES

Alam, S., Albareti, F. D., Allende Prieto, C., et al. 2015, ApJS, 219, 12
Arnaud, K. A. 1996, in ASP Conf. Ser. 101, Astronomical Data Analysis Software and Systems V, ed. G. H. Jacoby, & J. Barnes (San Francisco, CA: ASP), 17
Brandt, W. N., Schneider, S. P., Fan, X. H., et al. 2002, ApJ, 569, 5
Brightman, M., Silverman, J. D., Mainieri, V., et al. 2013, MNRAS, 433, 2485
Cash, W. 1979, ApJ, 228, 939
Fabian, A. C., Walker, S. A., Celotti, A., et al. 2014, MNRAS, 442, 81
Fan, X., Carilli, C. L., & Keating, B. 2006, ARA&A, 44, 415
Fan, X., Strauss, M. A., Gunn, J. E., et al. 1999, ApJL, 526, L57
Frey, S., Paragi, Z., Gurvits, L. I., Cseh, D., & Gabányi, K. É 2010, A&A, 524, A83
Fruscione, McDowell, J. C., Allen, G. E., et al. 2006, Proc. SPIE, 6270, 62701
Garmire, G. P., Bautz, M. W., Ford, P. G., Nousek, J. A., & Ricker, G. R. 2003, Proc. SPIE, 4851, 28
Gehrels, N. 1986, ApJ, 303, 336
Ghisellini, G., Haardt, F., Della, R. C., Volonteri, M., & Sbarrato, T. 2013, MNRAS, 432, 2818
Ghisellini, G., Tagliaferri, G., Sbarrato, T., & Gehrels, N. 2015, MNRAS, 450, 34
Gibson, R. R., Brandt, W. N., & Schneider, D. P. 2008, ApJ, 685, 773
Gregory, P. C., & Loredo, T. J. 1992, ApJ, 398, 146
Grupe, D., Mathur, S., Wilkes, B., & Osmer, P. 2006, ApJ, 131, 55
Hryniewicz, K., Czerny, B., Nikołajuk, M., & Kuraszkiewicz, J. 2010, MNRAS, 404, 2028
Jiang, L., McGreer, I. D., Fan, X., et al. 2015, AJ, 149, 188
Jin, C., Ward, M., & Done, C. 2012, MNRAS, 425, 907
Just, D. W., Brandt, W. N., Shemmer, O., et al. 2007, ApJ, 665, 1004
Kalberla, P. M. W., Burton, W. B., Hartmann, D., et al. 2005, A&A, 440, 775
Leighly, K. M. 1999, ApJS, 125, 317
Leighly, K. M., Halpern, J. P., Jenkins, E. B., & Casebeer, D. 2007, ApJS, 173, 1
Luo, B., Brandt, W. N., Hall, P. B., et al. 2015, ApJ, 805, 122
Lyons, L. 1991, A Practical Guide to Data Analysis for Physical Science Students (Cambridge: Cambridge Univ. Press)
Madau, P., Haardt, F., & Dotti, M. 2014, ApJ, 784, 38
Meusinger, H., & Balafkan, N. 2014, A&A, 568, A114
Moretti, A., Ballo, L., Braito, V., et al. 2014, A&A, 563, 46
Mortlock, D. J., Warren, S. J., Venemans, B. P., et al. 2011, Natur, 474, 616
Page, M. J., Simpson, C., Mortlock, D. J., et al. 2014, MNRAS, 440, 91
Park, T., Kashyap, V. L., Siemiginowska, A., et al. 2006, ApJ, 652, 610
Piconcelli, E., Jiminez-Bailon, E., Guinazzi, M., et al. 2005, A&A, 432, 15
Pounds, K. A., Done, C., & Osborne, J. P. 1995, MNRAS, 277, L5
Risaliti, G., & Lusso, E. 2015, ApJ, 815, 33
Risaliti, G., Young, M., & Elvis, M. 2009, ApJL, 700, L6
Romani, R. W., Sowards-Emmerd, D., Greenhill, L., & Michelson, P. 2004, ApJL, 610, L9
Sbarrato, T., Tagliaferri, G., Ghisellini, G., et al. 2013, ApJ, 777, 147
Shankar, F., Weinberg, D. H., & Miralda-Escudé, J. 2009, ApJ, 690, 20
Shemmer, O., Brandt, W. N., Anderson, S. F., et al. 2009, ApJ, 696, 580
Shemmer, O., Brandt, W. N., Netzer, H., Maiolino, R., & Kaspi, S. 2008, ApJ, 682, 81
Shemmer, O., Trakhtenbrot, B., Anderson, S. F., et al. 2010, ApJL, 722, L152
Steffen, A. T., Strateva, I., Brandt, W. N., et al. 2006, AJ, 131, 2826
Venemans, B. P., Findlay, J. R., Sutherland, W. J., et al. 2013, ApJ, 779, 24
Volonteri, M. 2010, A&ARv, 18, 279
Wang, J.-M., Watarai, K.-Y., & Mineshige, S. 2004, ApJ, 607, 107
Wang, F., Wu, X.-B., Fan, X., et al. 2016, ApJ, 819, 24
Wu, J., Brandt, W. N., Anderson, S. F., et al. 2012, ApJ, 747, 10
Wu, X.-B., Wang, F., Fan, X., et al. 2015, Natur, 518, 512
Yang, Q. X., Xie, F. G., Yuan, F., et al. 2015, MNRAS, 447, 1692
Young, M., Elvis, M., & Risaliti, G. 2009, ApJS, 183, 17